




## Co-Treatment with Sulforaphane and Nano-Metformin Molecules Accelerates Apoptosis in HER2+ Breast Cancer Cells by Inhibiting Key Molecules

A. Keshandehghan, S. Nikkhah, H. Tahermansouri, S. Heidari-Keshel & M. Gardaneh

To cite this article: A. Keshandehghan, S. Nikkhah, H. Tahermansouri, S. Heidari-Keshel & M. Gardaneh (2020) Co-Treatment with Sulforaphane and Nano-Metformin Molecules Accelerates Apoptosis in HER2+ Breast Cancer Cells by Inhibiting Key Molecules, *Nutrition and Cancer*, 72:5, 835-848, DOI: [10.1080/01635581.2019.1655073](https://doi.org/10.1080/01635581.2019.1655073)

To link to this article: <https://doi.org/10.1080/01635581.2019.1655073>

 View supplementary material 

 Published online: 02 Sep 2019.

 Submit your article to this journal 

 Article views: 51

 View related articles 

 View Crossmark data 



## Co-Treatment with Sulforaphane and Nano-Metformin Molecules Accelerates Apoptosis in HER2+ Breast Cancer Cells by Inhibiting Key Molecules

A. Keshandehghan<sup>a</sup>, S. Nikkhab<sup>b</sup>, H. Tahermansouri<sup>b</sup>, S. Heidari-Keshel<sup>c</sup>, and M. Gardaneh<sup>a</sup>

<sup>a</sup>Department of Stem Cells and Regenerative Medicine, Division of Medical Biotechnology, National Institute of Genetic Engineering and Biotechnology, Tehran, Iran; <sup>b</sup>Department of Chemistry, Ayatollah Amoli Branch, Islamic Azad University, Amol, Iran; <sup>c</sup>Department of Tissue Engineering and Applied Cell Sciences, School of Advanced Technologies in Medicine, Shahid Beheshti University of Medical Sciences, Tehran, Iran

### ABSTRACT

Breast cancer cell lines MCF-10, MCF-7 and BT-474 expressing various levels of HER2 were examined for their response to treatment with sulforaphane (SLFN), metformin (MTFN), Nano-MTFN or combinations. Direct correlation was found between SLFN effect on cell death and HER2 levels. Bioinformatic studies suggested the possibility of additive co-effects on cell fate by SLFN-MTFN co-treatment. This co-treatment specially with SLFN + Nano-MTFN significantly affected the survival of the cells and killed more BT-474 cells than the other two. Cell sensitivity to SLFN-MTFN combination correlated with HER2 expression levels. RT-PCR showed that parallel with cell death, expression of BCL-2, SRC, WNT1,  $\beta$ -catenin and CD44 are diminished, whereas BAX levels are elevated significantly. Cell co-staining indicated that apoptosis percent correlates with cell death following different treatments. We also found that cell death induced by SLFN-MTFN co-treatment is in direct correlation with HER2 levels and increased cell death correlates directly with BAX levels but inversely with levels of cancer stem cell (CSC) signaling genes and CD44. In conclusion, our data indicate that SLFN and MTFN can reduce cancer cell viability via both collaborative and differential effects and suggest that MTFN increases SLFN effectiveness by targeting common molecules/pathways downstream of HER2 and key for CSC signaling.

### ARTICLE HISTORY

Received 18 July 2019  
Accepted 7 August 2019

### Introduction

Cancer stem cells (CSCs) in breast cancer (BC) are identified by expression of specific markers that include CD44 and ALDH (1). The CSC population within a given BC tumor not only promotes tumor mass development but also is considered the main source of cancer drug resistance as they express ALDH a feature of EMT, which is a critical phenotypic switch associated with enhanced capacity of cells for invasion, metastasis, and chemoresistance (2). Current chemo and radiotherapy are unable to kill CSCs (3).


Defects in receptor tyrosine kinase (RTK) signaling is a major cause for cancer development (4). Overexpression and/or overactivity of molecular switches between RET and ER $\alpha$  in BC play a critical role in resistance to hormone therapy (5,6). SRC is an important example of nonmembrane tyrosine kinases which compensates the defects caused on other

switches. It also activates CSC receptors MET and FAK and make CSCs more aggressive and metastatic (7). We have previously reviewed interactions between RTKs in BC (8). Heterodimerization between HER1-HER2 results in Wnt-HER2 interaction that activates Wnt pathway via  $\beta$ -catenin phosphorylation in favor of CSC self-renewal (9). Overall, the interactions between various RTKs and molecular switches play a major role in resistance to tamoxifen as well as anti-HER2 antibody trastuzumab (TZMB). Inhibition of these interactions and inactivation of the switches involved could provide a chance for breaking such resistances and halting metastatic tumor growth.

Sulforaphane (SLFN) is an isothiocyanate found in broccoli sprouts (10) that has inhibitory and suppressive effects against cancer (11). SLFN moderates various cellular activities related to inhibition of transformed cells (11,12) including apoptosis induction and cell-cycle arrest (13). It also suppresses

**CONTACT** M. Gardaneh  [mossa65@nigeb.ac.ir](mailto:mossa65@nigeb.ac.ir), [mossabenis65@yahoo.com](mailto:mossabenis65@yahoo.com)  National Institute of Genetic Engineering and Biotechnology, Pazhoohesh Blvd, Tehran-Karaj HWY Kilometer 15, PO BOX 14965/161, Tehran-Iran.

Color versions of one or more of the figures in the article can be found online at [www.tandfonline.com/hnuc](http://www.tandfonline.com/hnuc).

 Supplemental data for this article can be accessed on the [publisher's website](http://publisher's website).

angiogenesis and metastasis via inhibiting specific molecules (12). SLFN prevents mammosphere formation by CSCs and downregulates their Wnt/ $\beta$ -catenin self-renewal pathway leading to reduced ALDH<sup>+</sup> CSC population within BC lines (14) and inhibited migration, invasion, clonogenicity, and in vivo tumorigenicity of xenografts via tumor-suppressive miR200c (15). Moreover, SLFN-mediated activation of miR-124 which targets IL-6R and STAT3 gene sequences (16) potentiates the low-dose anticancer properties of cisplatin. This is an indication of SLFN potential in sensitizing cancer cells to chemotherapy by killing CSCs. SLFN further causes elevated production of reactive oxygen species (ROS) that induce mitochondria-mediated apoptosis and along with other molecular changes mediate SLFN-induced suppression of growth and invasion (17,18).

Metformin (MTFN; N',N'-dimethylbiguanide hydrochloride) is the most commonly used medication in patients with type-II diabetes (19). MTFN can have antitumorigenic effects on BC specially that diabetic women have higher rate of BC incidence (20). The diabetic patients who consume MTFN are reportedly at lower risk of cancer (21) and show lower rate of mortality compared to their control counterparts who do not use the drug (22). Early-stage BC patients who receive MTFN fully respond to neoadjuvant therapy (23).

Metformin has two functional pathways: indirect effect (insulin-dependent) and direct effect (insulin-independent) (24). The indirect mechanism involves insulin receptor (IR) which is overexpressed in BC and together with IR/insulin-like growth factor-1R (IGF-1R) activation contributes to poor BC prognosis (25). MTFN reduces circulating insulin levels (26) and IGF-1R thereby reducing BC cell growth. MTFN administration in BC patients without diabetes reduces PKB/Akt and ERK1/2 phosphorylation (27). The direct effect of MTFN involves AMPK-dependent energy stress response that inhibits the mTOR-signaling pathway, thereby reducing protein synthesis and proliferation of cancer cells (28,29). It is largely believed that by doing this, MTFN causes reprogramming of cancer cell metabolism, thereby raising the efficacy of anticancer drugs (2). Due to this re-sensitizing property of MTFN, its combination with carboplatin, doxorubicin, and paclitaxel results in synergistic inhibition of cell proliferation in BC lines (30–32) including CSC killing and cancer cell chemo-sensitization (33–35).

Carbon nano-drugs are known as carbon nanomaterials (carbon nanotube and graphene) and show

outstanding characteristics that make them desirable tools for drug delivery. As a result, widespread research has been diverted toward cancer therapy and other biomedical utilities (36,37). Nevertheless, the medical and biological applications of carbon nanomaterials are limited due to their high hydrophobicity and low functionality. Hence, the functionalization of their surface with suitable chemical moieties can improve their applications so they can interact with anticancer drugs. Thus, widespread research has been dedicated to the functionalization of carbon nanomaterials, focusing on oxidation (38), cycloaddition (39), acylation (40) and amidation (41,42). Carbon nanotubes (CNTs) and graphene oxide (GO) carry several active oxygen-bearing groups including OH and COOH on their surface that promote chemical changes.

In search of possible convergent points or additive effects between SLFN and MTFN as two anti-tumorigenic compounds to maximize growth inhibition of BC cells and CSC populations, we examined how BC cell death can be induced by altering intracellular signaling pathways downstream of HER2 receptor. We first examined drug effects individually on cancer cell viability. We then combined MTFN with GO and MWCNT-COOH to generate GO-MTFN and MWCNT-MTFN before using them with SLFN in our co-treatment studies and correlating the findings with our gene expression data.

## Materials and Methods

### Cell Culture

Three BC cell lines, namely MCF-10, MCF-7, and BT-474, were cultured in Dulbecco's Modified Eagle Medium (DMEM) supplemented with 20% FBS and incubated in 37°C and 5% CO<sub>2</sub>. Horse serum substituted FBS in the case of MCF-10.

### Cell Treatment

Sulforaphane (Sigma) was diluted to 100  $\mu$ g/mL in DMSO. The cells were seeded in 96-well plates with 5000–7000 cells per well in 100–150  $\mu$ L medium and incubated for 24 hrs before treated with serial dilutions of SLFN. The treated cells were incubated for 8 hrs, followed by measuring cell viability by MTT assay, as we have described (43). The MTFN powder (Dr. Abidi Pharmaceuticals, Tehran) was dissolved in PBS to make 1 M stocks. Similar to SLFN, cell treatment was repeated with MTFN and viability data were used to determine the LD<sub>50</sub> of either drug.

**Table 1.** Primer sequences for RT-PCR.

Name		Primer sequence	Size (bp)	Anneal. temp	Accession #
HER2	F	CGCTGCTGGGAGAGAGTTC	676	52 °C × 45"	NM_001005862.1
	R	GGTTCTGGAAGACGCTGAGG			
BCL-2	F	GAACTGGGGGAGGATTGTGG	211	46 °C × 45"	NM_000633.2
	R	GAAATCAAACAGAGGCCGCA			
BAX	F	GTGGTTGGGTGAGACTCCTC	216	50 °C × 45"	NM_004324.3
	R	GCAGGGTAGATGAATCGGGG			
SRC	F	TGGAGCTCTGTGGGTCTCTG	141	48 °C × 45"	NM_198291.1
	R	AGCTCTCGACATAGACCGGG			
WNT-1	F	CTCTCTTCCCCTTTGTC	345	48 °C × 45"	NM_005430.3
	R	AACTCGTGGCTCTGTATCC			
β-CATENIN	F	GCGTGGACAATGGCTACTCAAG	516	48 °C × 45"	NM_001014431.1
	R	TATTAACCACCACCTGGTCTCTC			
CD44	F	TGGCACCCGCTATGTCGAG	214	48 °C × 45"	NM_000610.3
	R	GTAGCAGGGATTCTGTCTG			
GAPDH	F R	GTCTCCTCTGACTTCAACAGCG ACCACCTGTTGCTGTAGCCAA	130	56 °C × 45"	NM_002046

### Production of Nano-Metformin

We used two Nano particles to combine with MTFN: 1. MWCNT-COOH: %95 purity, OD: 10-30 nm, Length: 0.5–2 μm, Neutrino Co., Ltd., and 2. Graphene oxide nanoplatelets (99%, Thickness 3.4–7 nm with 6–10 Layers). We determined MTFN concentration using Unico UV-2100 Model variable-wavelength UV-Vis spectrophotometry. The SEM images of MTFN were prepared by Field emission scanning electron microscope (FESEM) using MIRA3\TESCAN-XMU model. The FESEM method was further applied to examine the morphology of MWCNT molecules and prepare SEM scans of the Nano-MTFN combinations. These FESEM images were prepared using thermogravimetric analysis (TGA) (Netzsch TG 209 F1 Iris1) in atmospheric nitrogen (10 °C/min).

In order to prepare MWCNT-MTFN and GO-MTFN, 400 mg of each compound was dissolved in 30 mL SOCl<sub>2</sub> and 1 mL DMF and incubated in 70 °C for 24 hrs under reflux conditions. Next, the remaining SOCl<sub>2</sub> was separated using pressure to obtain acylchloride-functionalized MWCNT (MWCNT-COCl) or GO (GO-COCl). Finally, the products were mixed with 700 mg MTFN in 40 mL DMSO and stirred in 100 °C for 72 hrs. The mix was then cooled to room temperature and rinsed with DMSO and tetrahydrofuran. The produced dark solid object was dried in vacuum for 8 hrs before use.

### Evaluation of SLFN-MTFN Co-Effect

Once the LD<sub>50</sub> of each drug was determined, we applied Design Expert as software of our choice to determine the possible interactions between the two drugs and their co-treatment effect of each cell line. We first treated the cells with doses of each drug below its LD<sub>50</sub>. This step determined approximate

doses of the drugs that, when co-applied, can kill 50% of the co-treated cells. Upon examination of these doses, we treated the cells with this range of doses in order to determine the exact LD<sub>50</sub> for co-treatment.

### Cell Co-Staining and Live Cell Count

We followed our reported method to co-stain treated cell samples with acridine orange (AO) and ethidium bromide (EB) to measure the percent of viable cells (44). Cell samples were suspended in PBS at a normal counting concentration from which we mixed 50 μL with 50 μL of the stain in 96-well plates before capturing the cell images under fluorescent microscope coupled with a Nikon digital camera. From the captured microscopic fields, we selected six random fields per well and counted an average of 120 cells for each cell group in triplicates (three wells per group). Green cells and orange cells were considered, respectively, as live and dead cells. The data collected from three independent experiments were then expressed as percent of live cells by dividing the number of live cells by the number of total cells counted (live + dead).

### RNA Extraction and Reverse Transcription (RT) PCR

Extraction of RNA and RT-PCR were carried out as reported (45). The primer pairs we used for each gene candidate are shown in Table 1. PCRs were carried out for 30 cycles consisting of denaturation at 95 °C for 45", annealing at various temperatures. Gel electrophoresis and band intensity measurement were duplicated as reported (45).

### Statistical Analyses

Data in the figures are represented as the mean ± standard error of the mean (SEM) of three or more

separate experiments. Student's *t*-test was used to analyze differences between two groups. Differences among three or more groups were analyzed by one-way analysis of variance (ANOVA), followed by a *post hoc* Duncan multiple-comparisons test ( $P < 0.05$ , statistically significant;  $P < 0.01$  or  $P < 0.001$ , highly significant). For correlations analyses (Correlations-Pearson, 2-tailed), we used triplicate data of each experimental set and compared relevant pairs as we have reported (44,45).

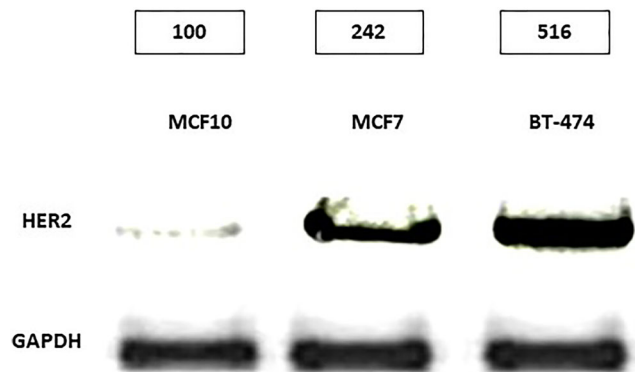


**Figure 1.** HER2 mRNA expression in BC cell lines. The figures show fold expression of Her2 that were obtained as outlined in Methods.

## Results

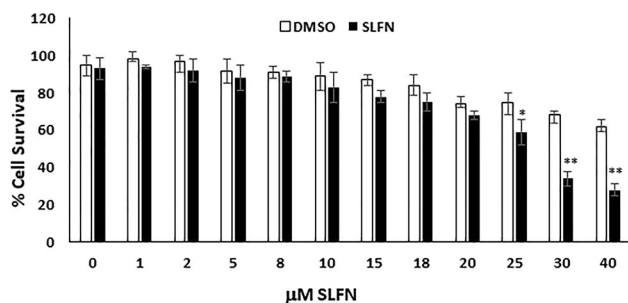
### 1. HER2 Gene Expression among BC Cell Lines

Our selected BC cell lines MCF-10, MCF-7, and BT-474 with various expression profiles were cultured and perpetuated in the lab. Total RNA was extracted from each cell line and subjected to RT-PCR. HER2 gene amplification was carried out as reported (46). Figure 1 indicates that BT-474 has the highest levels of HER2 gene expression. Band intensities were measured that showed HER2 mRNA levels in BT-474 cells is 5-fold more than in MCF-10 cells, whereas this figure in MCF-7 stood at 2.5-fold.

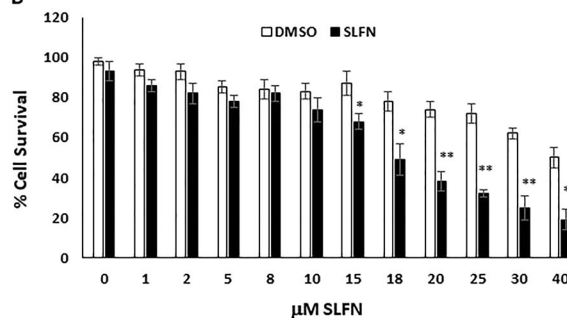
### 2. Sulforaphane-Induced BC Cell Death

Figure 2 shows the effect of SLFN treatment on survival of BC cell lines. We normalized the results of SLFN treatment to those of drug solvent DMSO as our control and determined 30  $\mu\text{M}$  as the LD<sub>50</sub> of the drug for MCF-10 cells (Fig. 2(A)). We found that this cell line tends to resist against SLFN effect and respond only to elevated doses of the drug. In contrast, the LD<sub>50</sub> of SLFN for MCF-7 was 22  $\mu\text{M}$ . The results showed that this cell line moderately resists SLFN effect but steadily responds to increasing

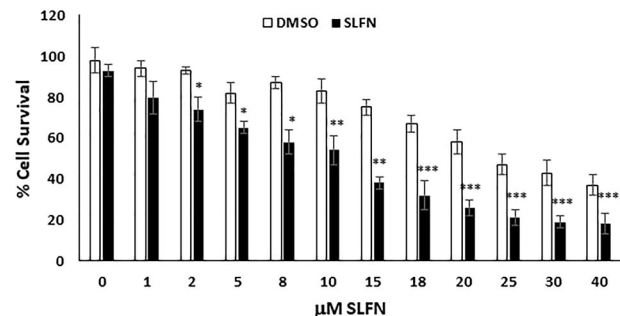
#### A MCF-10



#### B MCF-7



#### C BT-474



#### D

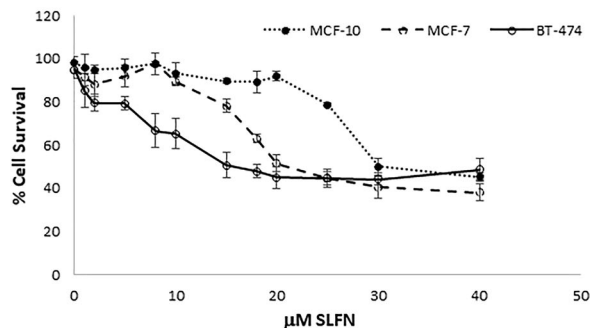


**Figure 2.** The effect of sulforaphane on BC cell lines. In this and subsequent figures, each column in graphs A-C and each line in graph D represent an average of three independent experiments. A. MCF-10, B. MCF-7, C. BT-474, D. graphs A-C normalized to DMSO. Symbols \* ( $P < 0.05$ ), \*\* ( $P < 0.01$ ), or \*\*\* ( $P < 0.001$ ) indicate statistical differences between each sample treated with SLFN and the same sample treated with DMSO.

concentrations of SLFN (Fig. 2(B)). Treatment of BT-474, on the other hand, showed LD<sub>50</sub> for SLFN was 14 μM (Fig. 2(C)). The cells failed to resist higher doses of SLFN and died extensively. Upon normalization of the results for each cell line, we found that BT-474 shows the highest levels of response to SLFN, whereas MCF-10 is the least sensitive line to the drug (Fig. 2(D)).

### 3. Construction of Nano-Metformin Compounds

The synthesis route of MWCNT-MTFN and GO-MTFN after treatment of MWCNT-COOH and GO with MTFN is shown in Fig. 3(A). The products were characterized by Fourier transform infrared spectroscopy (FT-IR), Thermogravimetric analysis (TGA), derivative thermogravimetric (DTG), and scanning electron microscope (SEM). TGA is a valuable tool to characterize the modified carbon nanomaterials which presents quantitative and useful information concerning the modification of MWCNTs and GO. According to Fig. 3(B) that indicates the TGA curve of MWCNT-COOH is almost thermally stable, the weight loss before decomposition of MWCNTs can be used to estimate the quantity of various groups attached to nanotube. TGA curve of MWCNT-met displays 51.97% mass loss about 120–260 °C owing to the decomposition of metformin groups as compared to TGA of MTFN. In addition, our calculations showed about 2.69 mg MTFN attached to MWCNT in the MWCNT-MTFN (5.17 mg of MWCNT-MTFN was used for test). On the other hand, TGA curve of GO displays 8.86% mass loss below 120 °C which can be assigned to the evaporation of adsorbed water on the GO. A rapid mass loss occurred at around 140–210 °C with a weight loss about 11.51% arising from the removal of the oxygen-bearing functional groups. Also, it shows a gradual trend in decomposition from 210–380 °C with a weight loss of 25% that can be assigned to further removal of functional groups (probably carboxylic groups). In TGA of GO-MTFN, one decomposition at around 120–700 °C with a weight loss of 27.67% is observable which can be assigned to decomposition of MTFN groups as compared to TGA of MTFN. On the basis, there are about 1.63 mg MTFN on GO-MTFN (5.9 mg of GO-MTFN was used for test). DTG curve provides further evidence for modification. In Fig. 3(C), the peak at 230 for MWCNT-MTFN and 205 °C for GO-MTFN could be attributed to the decomposition of the MTFN (as compared to DTG of MTFN). These results indicate

that MTFN has been located onto the carbon nanomaterials.

Field emission scanning electron microscope (FESEM) images of carbon nanomaterials were indicated in Fig. 3(D,E). As shown in these figures, GO sheets clearly present a sheet-like structure with large thickness, smooth surface, and wrinkled edge. In addition, the SEM image of MWCNT-COOH shows a cylindrical, rope-like shapes highly tangled and agglomerated with each other. After functionalization with MTFN to form MWCNT-MTFN and GO-MTFN, we collected interesting images: as shown in Fig. 3(D,E), substantial number of MTFN molecules were located on graphene and MWCNT that confirms the functionalization between MTFN and the carbon materials.

### 4. The Effect of Metformin and Nano-Metformin on the Survival of Cancer Cells

All three BC cell lines were treated with serial concentrations of the compounds followed by measuring their viability. As shown in Fig. 4, MCF-10 cells showed sensitivity when treated with high doses of MTFN and MWCNT-MTFN so the LD<sub>50</sub> for MTFN alone and MWCNT-MTFN became 50 mM, whereas this figure was 48 and 42 mM, respectively, for MCF-7 and BT-474.

### 5. Bioinformatic Studies on Sulforaphane-Metformin Co-Treatment

As outlined in Methods, the bioinformatic section of our study was carried out using the Design Expert software. After examining the obtained model, the software produced graphs and its data showed that SLFN and MTFN are unlikely to synergize on particular molecules or cell-signaling pathways (Supplement Figure), but this observation does not exclude their cooperative effects on cancer cells.

### 6. The Additive Co-Effect of Sulforaphane and Metformin or Nano-Metformin on Cancer Cell Survival

Based on our findings in silico and reports on the individual anticancer treatment of either compound, we concluded that the SLFN-MTFN minimum co-effect on cell lines will be additive. To test this notion, we first co-treated all three cell lines with SLFN + MTFN or SLFN + MWCNT-MTFN. Here, we used LD<sub>50</sub> of SLFN and increasing concentrations of

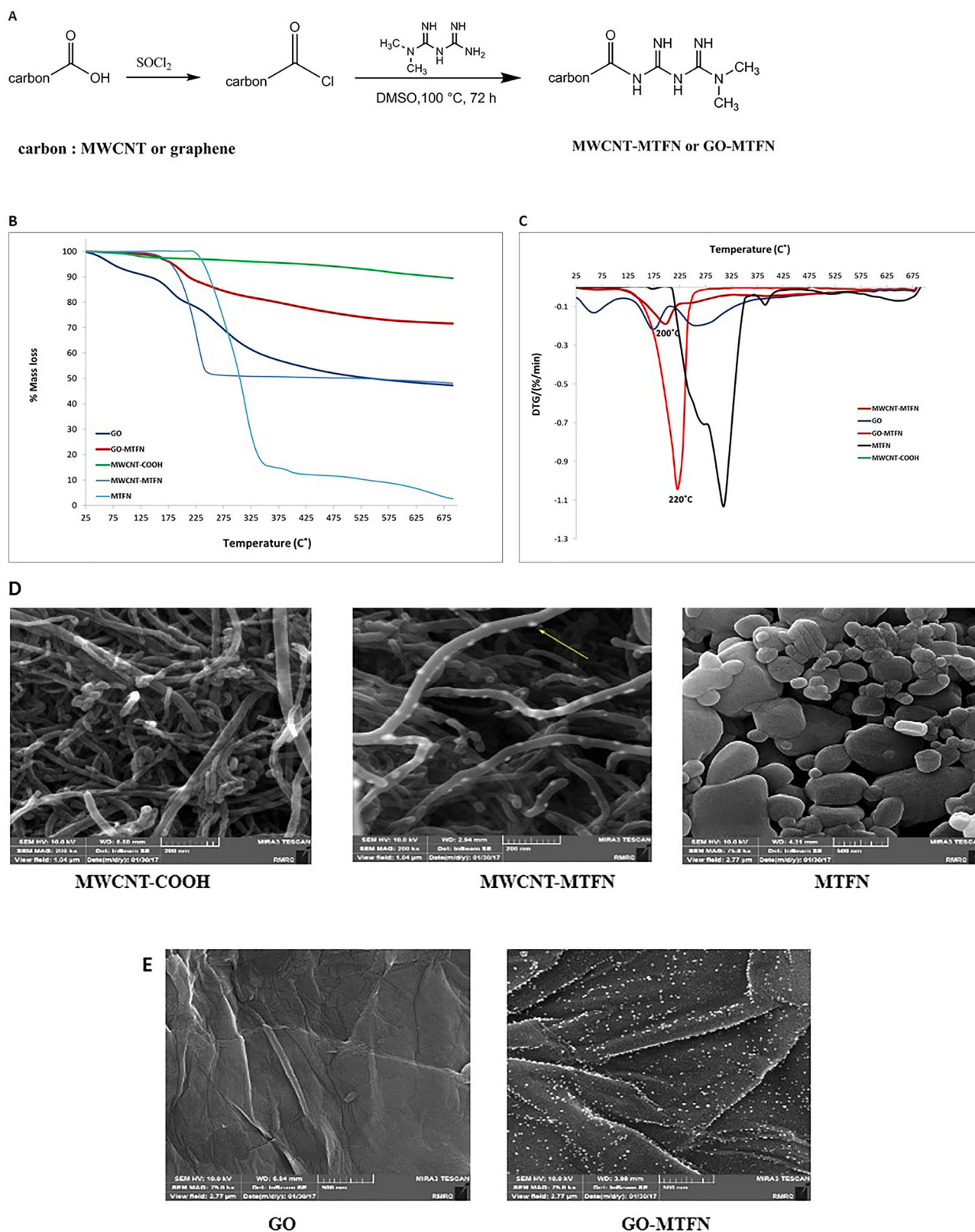


**Figure 3.** Synthesis of nan-metformin compounds. A. steps of chemical synthesis. B and C. TGA and DTG curves of the modified nano-carbon compounds. D and E. Electron microscopic images of synthesized nano-MTFN compounds. See text for more details.

MTFN. As shown in Fig. 5(A), 15 mM MTFN reduced viability of SLFN-treated MCF-7 and BT-474, respectively, by 12% ( $P < 0.05$ ) and 24% ( $P < 0.01$ ). When we

used 30 mM MTFN, viability of MCF-7 and BT-474 were reduced by a further 6%. Using 60 mM MTFN, MCF-7, and BT-474 cell viabilities stood, respectively,

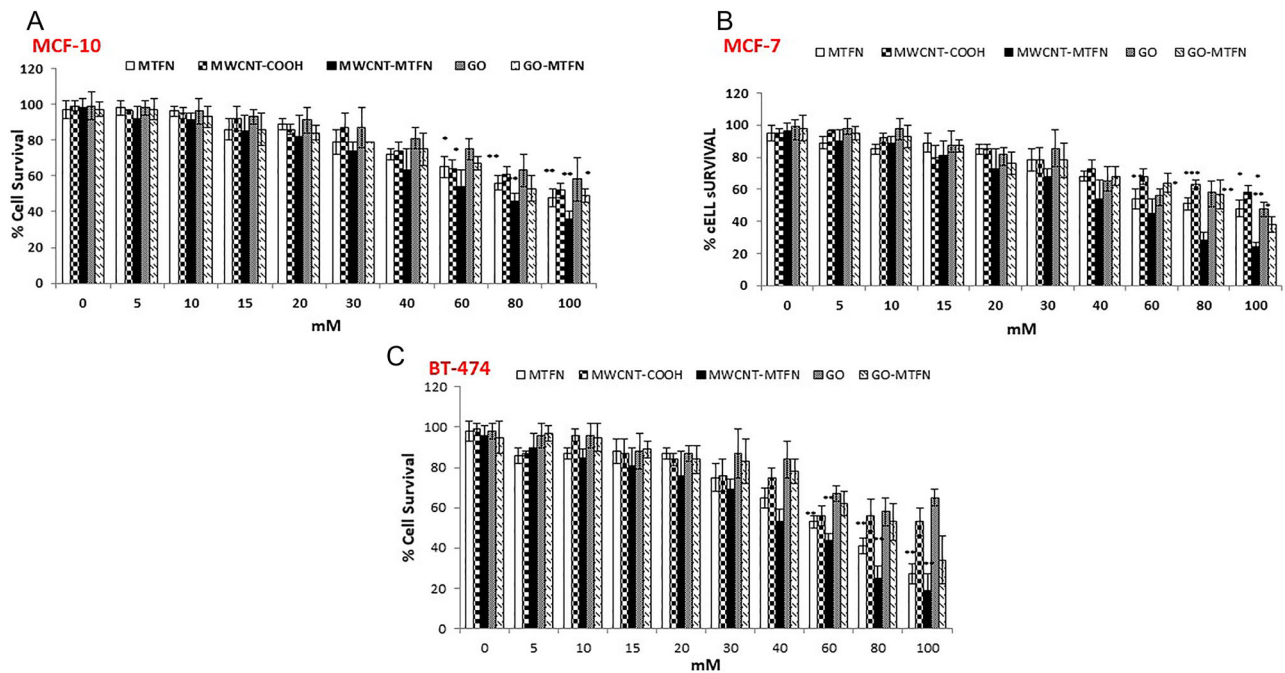


**Figure 4.** The effect of metformin and nano-metformin on BC cell lines. A. MCF-10, B. MCF-7 and C. BT-474. Symbol \*, \*\*, or \*\*\* indicates statistical differences between each treated sample and its equivalent in untreated control (0) group.

at 20% and 11%. All reductions were statistically significant (Fig. 5(A),  $P < 0.05$ ). These results suggested correlations between HER2 expression levels and the antisurvival efficacy of SLFN + MTFN combination.

Since BT-474 showed more vulnerability toward drug treatment, this line was further treated once with half  $LD_{50}$  of SLFN ( $7\mu\text{M}$ ) and once with full  $LD_{50}$  of the compound ( $14\mu\text{M}$ ), and in parallel, with serial concentrations of MTFN and or MWCNT-MTFN for 8 hours. Our initial assessment to compare the efficacy of MWCNT-MTFN and GO-MTFN indicated that the former acts better in potentiating MTFN against cancer cells and so we discontinued using GO-MTFN in our study. Measurement of cell viability showed that the increasing doses of MTFN enhance cell response to SLFN, so that 15 mM MTFN together with SLFN significantly increased cell death (Fig. 5(B),  $P < 0.05$ ). Increase in MTFN dose-accelerated cell death so that 60 mM MTFN plus half  $LD_{50}$  of SLFN killed 46% of the cells, highly significant rate compared to when we used  $7\mu\text{M}$  SLFN alone ( $P < 0.01$ ). The effect of MTFN on cell death became more pronounced when combined with nanotubes so that 60 mM MWCNT-MTFN reduced viability to 11%, significantly down from the group treated with half dose SLFN alone ( $P < 0.01$ ) and the one treated with full-dose SLFN alone ( $P < 0.05$ ). In fact, MTFN presence sensitizes the cells to SLFN effect so that, for example, 15 mM MTFN +  $7\mu\text{M}$  SLFN reduces cell viability to 28% compared to 63% in the presence of  $7\mu\text{M}$  SLFN alone ( $P < 0.01$ ).

The figure stood at 20% when we replaced MTFN with MWCNT-MTFN. We concluded that MTFN presence sensitizes the cells to SLFN effect, MWCNT-MTFN acts more efficiently than MTFN alone and this cell response increases dose dependently.

### 7. The Additive Co-Effect of Sulforaphane and Metformin on Gene Expression

We examined changes in mRNA expression of key genes in treated BT-474 (Fig. 6). These genes included the antiapoptotic BCL-2, BAX as pro-apoptotic molecule, SRC acting as molecular switch in receptor tyrosine kinase signaling pathways, Wnt-1,  $\beta$ -Catenin as two key molecules involved in cancer stem cell signaling and CD44 as a dominant receptor in BC stem cells (Fig. 6(A)). Fig. 6(B) shows changes in the expression of these candidates by comparing their band intensity, as outlined in Methods. Here, we used  $14\mu\text{M}$  SLFN as its  $LD_{50}$  for BT-474 and 40 mM MTFN or MWCNT-MTFN. These results indicate that pro-apoptotic BAX in the presence of SLFN, SLFN + MTFN and most notably SLFN + MWCNT-MTFN has had the highest level of expression, whereas all other gene candidates show the least levels of expression. These changes in co-treated samples were significant ( $P < 0.05$ ) to highly significant ( $P < 0.01$  or 0.001) compared to untreated samples or SLFN-treated ones (See Fig. 6(B)). Furthermore, comparison between each cell group co-treated with



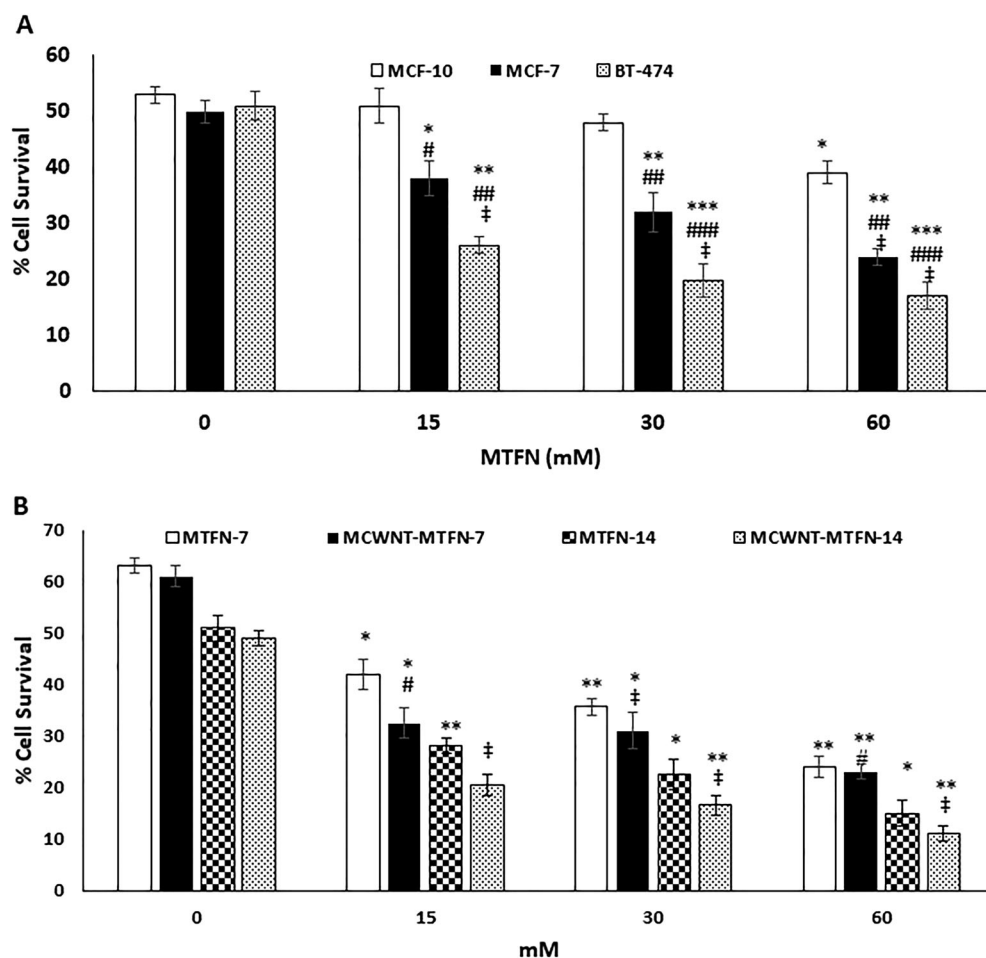


**Figure 5.** The effect of co-treatments on survival of BC cell line BT-474. **A.** cell groups treated with increasing concentrations of metformin. Symbol \*, \*\* or \*\*\* represents statistical differences between every sample and its corresponding one in untreated control (0) group. Symbol #, ## or ### shows differences between every sample and MCF-10 in the same group, and symbol †, †† or ††† compares BT-474 to MCF-7 in the same group. **B.** Beside SLFN, as the main drug compound, serial doses of metformin and nano-metformin were applied in co-treatment. Symbol \*, \*\* or \*\*\* indicates statistical differences between each column and its untreated control, whereas #, ##, or ### compares each column and the MTFN-7 column in its own group, and †, †† or ††† shows differences between each column and MWCNT-MET-14 within the same group.

SLFN + MCWNT-MTFN and its single treated counterpart indicate significant differences in expression of gene candidates ( $P < 0.05$ ). This difference is detected even compared with SLFN + MTFN highlighting the importance of nanotubes in potentiating the effect of MTFN.

### 8. Sulforaphane-Induced Promotion of Apoptotic Morphologies

We have previously reported detection of apoptotic morphology via cell co-staining using AO/EB (39,40). We applied the same method to detect apoptosis in our treated cells in the current study (Fig. 7(A)). Quantitation analysis showed that 24% of BT-474 cells treated with 7  $\mu$ M SLFN undergo apoptosis (Fig. 7(B),  $P < 0.05$ ). This figure increased to 30% when SLFN was accompanied by 40 mM MTFN and to 51% by

40 mM MWCNT-MTFN ( $P < 0.01$ ). This latest figure was highly significant compared to the apoptosis rate produced by SLFN + MTFN co-treatment ( $P < 0.05$ ).

### 9. Correlation Studies

We used SPSS, V. 17 to compare our data for correlation. Our correlation analyses shown in Table 2 indicates that the survival rate of cancer cells treated with SFN, SLFN + MTFN, and/or SLFN + MWCNT-MTFN inversely correlates with HER2 mRNA levels (for comparison, the increasing rate of HER2 expression from all three cell lines was taken to account). Comparison between BT-474 survival rate and mRNA of key molecules indicate that cell survival rate correlates directly with expression levels of pro-apoptotic BAX but inversely with the expression levels of other gene candidates we examined that are involved in

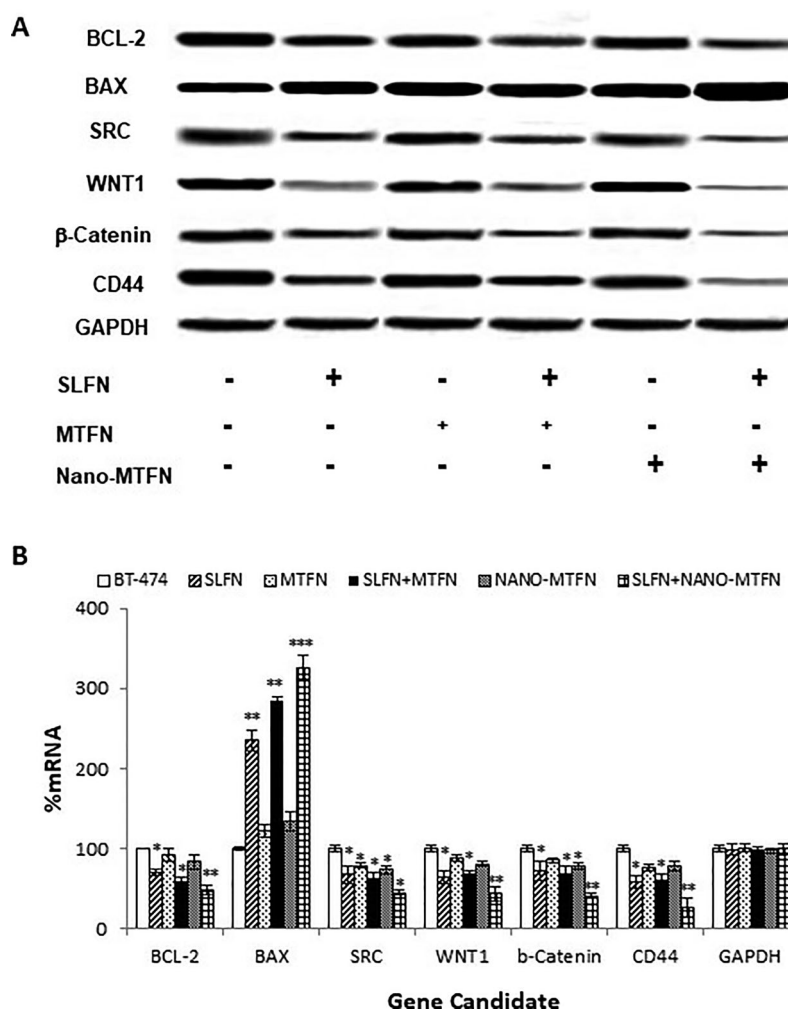


**Figure 6.** The effect of drugs on expression of key genes. **A.** Gel electrophoresis image of RT-PCR products. Total RNA was collected from cell groups treated with SLFN, MTFN, MWCNT-MTFN or co-treated. **B.** A graph of quantitative gene expression obtained by analyzing bands of the image in **A.** Symbol \*, \*\* or \*\*\* indicates statistical differences between each sample of treated cells and its untreated equivalent. Symbol † compares each co-treated sample with the one treated with SLFN alone, whereas # shows differences between each co-treated sample with the one treated with MTFN alone or with MWCNT-MTFN. Symbol ‡ or †† shows differences between SLFN + MWCNT-MTFN and SLFN + MTFN samples.

survival and growth of cancer cells and cancer stem cells. Specifically, BT-474 treated with SLFN or co-treated with SLFN + MTFN or SLFN + MWCNT-MTFN that showed the lowest rate of survival expressed the least levels of BCL-2, WNT-1, SRC,  $\beta$ -catenin and CD44 and this inverse correlation was significant in each case (Table 2,  $P < 0.05$ ).

## Discussion

A solution to drug resistance and to deadly consequences of cancer recurrence post-treatment is to apply adjuvant therapies in which chemotherapy drugs are combined with sensitizing compounds. SLFN and MTFN both are effective against CSCs as the main source of chemoresistance and EMT as a critical step in tumor progression towards metastasis.

In this study, we examined the co-effects of SLFN and MTFN on BC cell lines with different HER2 signaling profiles. We found that while each compound individually affects common molecules involved in BC cell growth and proliferation, their additive effects can be more profound. This was shown in our co-treated samples as we monitored significant changes first in cell viability and second in expression of key molecules and receptors involved in signaling cell growth, proliferation and cancer progression. Next, we combined MTFN with nanocarbon structures that potentiated the net anti-tumorigenic effects of our co-treatment. The data we collected from various analyses were matched pair to pair and indicated correlations between key parameters we studied.

Clinical therapies using anti-HER2 antibodies such as TZMB or lapatinib often end up with antibody

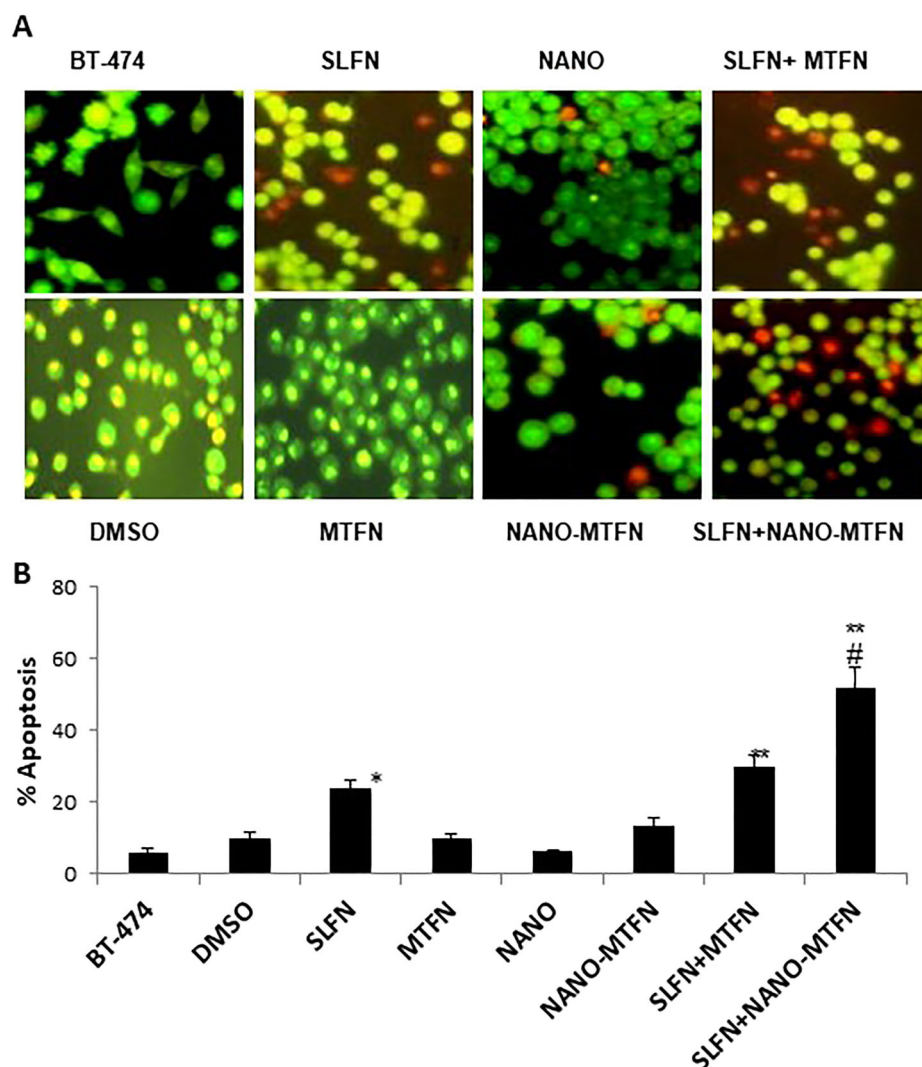


**Figure 7. Apoptotic morphology of treated BT-474 cells.** A. cells co-stained with acridine orange and ethidium bromide. Magnification: 200X. B. A graph representing percent of apoptosis (see Methods). Symbol \*\* compares statistical differences between each treated sample and the control (DMSO), whereas symbol # shows differences between SLFN + MWCNT-MTFN and SLFN + MTFN.

resistances. Co-targeting HER2 and some downstream signaling molecules including those of CSC renewal and proliferation could provide effective solutions. To this end, we selected SLFN and MTFN as two antitumorigenic antiresistance compounds. As an example, continuous treatment of TZMB-resistant BC patients, who carry loss of PTEN function, with the antibody transforms HER2<sup>+</sup>PTEN<sup>-</sup> BC to triple-negative BC (TNBC) (47). The cancer cells also become dependent on IL-6/STAT3/NF- $\kappa$ B-positive feedback loop. However, SLFN prevents TZMB-resistant cells from switching to TNBC phenotype by inhibiting the loop and suppressing production of IL-6 and translocation and transcriptional activity of NF- $\kappa$ B. SLFN also significantly reduces the CSC population in re-implanted xenograft models of BC (47). These observations emphasize the potential of SLFN in therapy of TZMB-

resistant BC tumors. As such, we selected three cell lines expressing various HER2 levels to examine the effect of SLFN on them. Our findings show that SLFN suppresses BC cell viability dose-dependently as well as according to HER2 levels. The effect of the compound on HER2-amplifying BT-474 cells was indeed more significant requiring less doses of the compound to affect the same rate of viability compared to the other two lines.

MTFN *per se*, on the other hand, is considered a drug sensitizer for cancer cells. In HER2-amplifying BC cell lines, MTFN downregulates cell growth and enhances apoptosis by inhibiting HSP90 (48). In hormone- or antibody-resistant TNBC patients, MTFN can act as an effective adjuvant therapy where STAT3 regulates its activity (49). The drug synergizes with doxorubicin to reverse drug resistance by

**Table 2.** Correlations studies.

	HER2 levels	SR (S)	SR (S + M)	SR (S + NM)	BCL-2	BAX	SRC	W/C	CD44	Ap (%)
HER2 Levels	100									
SR (S)	-97.8*	100								
SR (S + M)	-98.9*	NA	100							
SR (S + NM)	-99.3**	NA	NA	100						
BCL-2	NA	95	96.4	98.5*	100					
BAX	NA	99.5**	98.3**	NA	NA	100				
SRC	NA	99.3*	99.5**	99.8**	NA	NA	100			
W/C	NA	99.3*	99.5*	99.8**	NA	NA	NA	100		
CD44	NA	95.8	96.9	99.3*	NA	NA	NA	NA	100	
Ap (%)	NA	-96	-98	-99.3*	-97.3	98.8	-97.9	-99.1*	-98.9*	100

Note 1: \*, \*\* Correlation is significant at 0.05 (\*) or 0.01 levels (\*\*\*) (2-tailed). Note 2: NA, not applicable. Her2 correlations were measured based on its trend of expression in the 3 breast cancer cell lines (see Figure 3-1), whereas all other correlations were made based on the data collected from BT-474 cells only. Ap, apoptosis, M, metformin, NM, nano-metformin, S, sulforaphane, SR, Survival Rate, W/C, WNT/ $\beta$ -Catenin.

downregulating MDR1 (50). It also enhances the efficacy of emtansine (anti-HER2 TZMB attached to anti-tubulin DM1) in treating HER2-positive metastatic BC via upregulating Caveolin-1 (51). As for CSCs, MTFN reduces the number of ALDH<sup>+</sup> cells within BC cell populations (52) and indeed selectively kills CSCs in breast tumors (34) by regulating EMT transition (53). The compound effectively overcomes TZMB resistance by killing CSCs (54) and inhibiting interactions between HER2 and IGFR-1 (55). Systemic administration of MTFN extends life span and delays spontaneous BC development in MMTV-HER2 transgenic mice (56,57) while inhibiting a tumor-initiating HER2-positive subpopulation of mouse mammary tumors by downregulating expression/activity of HER2 and other key factors (58). This study suggests that increased HER2 expression and activity in CSC/tumor-initiating tumorsphere cells promotes self-renewal and proliferation and renders the cells more responsive to MTFN effects. Therefore, we selected MTFN to examine its effect on HER2-amplifying BC cells and how it can sensitize the cells to SLFN. First, we subjected our cell lines to combined treatment with SLFN + MTFN in order to find if there will be significant increase of co-effect on cell viability. We found that the more HER2 mRNA was expressed, the more profoundly the co-treatment affected cell viability. Therefore, we focused on HER2-amplifying BT-474 cells which showed highly significant response to SLFN + MTFN co-treatment. We concluded that high level presence of HER2 renders the cells susceptible to our co-treatment.

As for molecular mechanisms of this co-effect, our bioinformatic analysis did not favor synergistic effects by SLFN and MTFN but also did not exclude their additive effects. Therefore, either drug may function on a particular molecule or pathway via its distinct mechanism of action. Our PCR analysis indicated that expression of pro-apoptotic BAX was significantly induced in co-treated cell samples, whereas all other

genes in favor of cancer cell survival and progression were downregulated significantly. We examined SRC as internal molecular switch downstream HER2 and various growth pathways, CSC renewal markers WNT1 and  $\beta$ -catenin as well as CSC receptor CD44. SLFN + MTFN co-treatment has had suppressing effect on all these molecules which, compared to single treatments, was significant.

We also applied MTFN-nanocarbon combination to this co-treatment. The Nano-MTFN compounds were constituted with uniform distribution of MTFN molecules on nanotubes as evidenced from our SEM images. Application of MWCNT-MTFN accelerated the effect on MTFN in sensitizing HER2<sup>+</sup> cells to SLFN effects as evidenced from both declining BT-474 cell viability and changes in gene expression. Such changes were found significant compared to SLFN + MTFN co-treatment. The fact that markers of CSC biology were dramatically reduced in our co-treated samples suggest that SLFN-MTFN combination might be applied in treatment modalities for suppression of drug resistance in tumors that do not respond to chemotherapy or antibody therapy particularly HER2<sup>+</sup> tumors. This notion requires *in vivo* investigations to be examined and proven.

Finally, our analyses indicated changes in HER2 mRNA levels, cell viability, expression of gene candidates, apoptosis rate and the combination of our drugs that we applied are elements in direct or inverse correlation with one another. The overall picture of these correlations highly confirms that SLFN and MTFN can, in concert, co-influence BC cell and CSC survival and that the use of nanostructures can accelerate this trend.

In conclusion, we examined the notion that SLFN and MTFN jointly have profound effect on BC cell viability and, due to their increasing impact in parallel with increase in HER2 levels, overcome resistance against anti-HER2 antibody therapies. Application of nanocarbons can enhance such co-influence. It is yet

to be seen if such co-effect is significant in tumors of BC patients in vivo. Mechanistically also, further exploration is needed to determine precise changes in BC cell growth pathways and CSC capacity to promote EMT, drug resistance and invasion with the role of noncoding RNA molecules in each turning point.

## Acknowledgment

This study was financially supported by a grant from National Institute of Genetic Engineering and Biotechnology (NIGEB) (Grant 502). We thank colleagues in NIGEB for their technical assistance and scientific advice.

## Disclosure Statement

The authors declare no conflict of interest.

## Author Contribution

MG planned the whole project to which he received grant, conceived and designed study experiments, and drafted the whole manuscript; AK carried out the cell molecular biology section of the experiments. HT designed the nano section of the study and supervised others to do nano experiments and interpreted data. SN and SHK conducted nano experiments and analyzed data. SHK further analyzed viability of cancer cells treated with nano particles. All authors contributed to paper writing with MG and HT frequently editing the manuscript. The authors have read and approved the final manuscript.

## References

1. Ali HR, Dawson SJ, Blows FM, Provenzano E, Pharoah PD, et al.: Cancer stem cell markers in breast cancer: pathological, clinical and prognostic significance. *Breast Cancer Res* **13**, R118, 2011. doi:10.1186/bcr3061.
2. Qu C, Zhang W, Zheng G, Zhang Z, Yin J, and He Z: Metformin reverses multidrug resistance and epithelial-mesenchymal transition (EMT) via activating AMP-activated protein kinase (AMPK) in human breast cancer cells. *Mol Cell Biochem* **386**, 63–71, 2014.
3. Korkaya H, and Wicha MS: HER-2, notch, and breast cancer stem cells: Targeting an axis of evil. *Clin Cancer Res* **15**, 1845–1847, 2009. doi: 10.1158/1078-0432.CCR-08-3087.
4. Sangwan V, and Park M: Receptor tyrosine kinases: role in cancer progression. *Curr Oncol* **13**, 191–193, 2006.
5. Morandi A, Plaza-Menacho I, and Isacke CM: RET in breast cancer: functional and therapeutic implications. *Trends Mol Med* **17**, 149–157, 2011. doi:10.1016/j.molmed.2010.12.007.
6. Nardone A, De Angelis C, Trivedi MV, Osborne CK, and Schiff R: The changing role of ER in endocrine resistance. *Breast* **24**, S60–S66, 2015. doi:10.1016/j.breast.2015.07.015.
7. Thakur R, Trivedi R, Rastogi N, Singh M, and Mishra DP: Inhibition of STAT3, FAK and Src mediated signaling reduces cancer stem cell load, tumorigenic potential and metastasis in breast cancer. *Sci Rep* **5**, 10194, 2015. doi:10.1038/srep10194.
8. Shojaei S, Gardaneh M, and Rahimi Shamabadi A: Rahimi Shamabadi A: Target points in trastuzumab resistance. *Int J Breast Cancer* **2012**, 761917, 2012. doi: 10.1155/2012/761917.
9. Finigan JH, Vasu VT, Thaikootathil JV, Mishra R, Shatat MA, et al. HER2 activation results in  $\beta$ -catenin-dependent changes in pulmonary epithelial permeability. *Am J Physiol* **308**, L199–207, 2014.
10. Zhang Y, Talalay P, Cho CG, and Posner GH: A major inducer of anticarcinogenic protective enzymes from broccoli: isolation and elucidation of structure. *Proc Natl Acad Sci USA* **89**, 2399–2403, 1992.
11. Clarke JD, Dashwood RH, and Ho E: Multi-targeted prevention of cancer by sulforaphane. *Cancer Lett* **269**, 291–304, 2008.
12. Zhang Y, and Tang L: Discovery and development of sulforaphane as a cancer chemopreventive phytochemical. *Acta Pharmacol Sin* **28**, 1343–1354, 2007.
13. Suppipat K, Park CS, Shen Y, Zhu X, and Lacorazza HD: Sulforaphane induces cell cycle arrest and apoptosis in acute lymphoblastic leukemia cells. *PLoS One* **7**, e51251, 2012. doi:10.1371/journal.pone.0051251
14. Li Y, Zhang T, Korkaya H, Liu S, Lee HF, et al. : Sulforaphane, a dietary component of broccoli/broccoli sprouts, inhibits breast cancer stem cells. *Clin Cancer Res* **16**, 2580–2590, 2010. doi:10.1158/1078-0432.CCR-09-2937.
15. Liu CM, Peng CY, Liao YW, Lu M, Tsai M, et al. Sulforaphane targets cancer stemness and tumor initiating properties in oral squamous cell carcinomas via miR-200c induction. *J Formos Med Assoc* **116**, 41–e48, 2017.
16. Wang X, Li Y, Dai Y, Liu Q, Ning S, et al. Sulforaphane improves chemotherapy efficacy by targeting cancer stem cell-like properties via the miR-124/IL-6R/STAT3 axis. *Sci Rep* **6**, 36796, 2016. doi:10.1038/srep36796.
17. Wang L, Tian Z, Yang Q, et al. Sulforaphane inhibits thyroid cancer cell growth and invasiveness through the reactive oxygen species-dependent pathway. *Oncotarget* **6**, 25917–25931, 2015. doi:10.18632/oncotarget.4542.
18. Miao Z, Yu F, Ren Y, and Yang J: d,l-Sulforaphane induces ROS-dependent apoptosis in human glioblastoma cells by inactivating STAT3 signaling pathway. *IJMS* **18**, 72, 2017. doi:10.3390/ijms18010072.
19. Pierotti MA, Berrino F, Gariboldi M, Melani C, Mogavero A, et al. Targeting metabolism for cancer treatment and prevention: metformin, an old drug with multi-faceted effects. *Oncogene* **32**, 1475–1487, 2013.
20. Larsson SC, Mantzoros CS, and Wolk A: Diabetes mellitus and risk of breast cancer: a meta-analysis. *Int J Cancer* **121**, 856–862, 2007.

21. Evans JM, Donnelly LA, Emslie-Smith AM, Alessi DR, and Morris AD: Metformin and reduced risk of cancer in diabetic patients. *BMJ* **330**, 1304–1305, 2005.
22. Bowker SL, Majumdar SR, Veugelers P, and Johnson JA: Increased cancer-related mortality for patients with type 2 diabetes who use sulfonylureas or insulin. *Diabetes Care* **29**, 254–258, 2006.
23. Jiralerspong S, Palla SL, Giordano SH, Meric-Bernstam F, Liedtke C, et al. Metformin and pathologic complete responses to neoadjuvant chemotherapy in diabetic patients with breast cancer. *J Clin Oncol* **27**, 3297–3302, 2009.
24. Queiroz EA, Puukila S, Eichler R, Sampaio SC, Forsyth HL, et al. Metformin induces apoptosis and cell cycle arrest mediated by oxidative stress, AMPK and FOXO3a in MCF-7 breast cancer cells. *PLoS One* **9**, e98207, 2014.
25. Mulligan AM, O'Malley FP, Ennis M, Fantus IG, and Goodwin PJ: Insulin receptor is an independent predictor of a favorable outcome in early stage breast cancer. *Breast Cancer Res Treat* **106**, 39–47, 2007.
26. Goodwin PJ, Pritchard KI, Ennis M, Clemons M, Graham M, et al. Insulin-lowering effects of metformin in women with early breast cancer. *Clin Breast Cancer* **8**, 501–505, 2008.
27. Dowling RJ, Niraula S, Chang MC, Done SJ, Ennis M, et al. Changes in insulin receptor signaling underlie neoadjuvant metformin administration in breast cancer: a prospective window of opportunity neoadjuvant study. *Breast Cancer Res* **17**, 32, 2015. doi:10.1186/s13058-015-0540-0.
28. Zakikhani M, Dowling R, Fantus IG, Sonenberg N, and Pollak M: Metformin is an AMP kinase-dependent growth inhibitor for breast cancer cells. *Cancer Res* **66**, 10269–10273, 2006. 15,
29. Dowling RJ, Zakikhani M, Fantus IG, Pollak M, and Sonenberg N: Metformin inhibits mammalian target of rapamycin-dependent translation initiation in breast cancer cells. *Cancer Res* **67**, 10804–10812, 2007.
30. Liu H, Scholz C, Zang C, Sclafani JH, Habel P, et al. Metformin and the mTOR inhibitor everolimus (RAD001) sensitize breast cancer cells to the cytotoxic effect of chemotherapeutic drugs in vitro. *Anticancer Res* **32**, 1627–1637, 2012.
31. Ma J, Guo Y, Chen S, Zhong C, Xue Y, et al. Metformin enhances tamoxifen-mediated tumor growth inhibition in ER-positive breast carcinoma. *BMC Cancer* **14**, 172, 2014.
32. Sanchez-Alvarez R, Martinez-Outschoorn UE, Lamb R, Hult J, Howell A, et al. Mitochondrial dysfunction in breast cancer cells prevents tumor growth: understanding chemoprevention with metformin. *Cell Cycle* **12**, 172–182, 2013.
33. Davies G, Lobanova L, Dawicki W, Groot G, Gordon JR, et al. Metformin inhibits the development, and promotes the resensitization, of treatment-resistant breast cancer. *PLoS One* **12**, e0187191, 2017. doi:10.1371/journal.pone.0187191
34. Hirsch HA, Iliopoulos D, Tsihchlis PN, and Struhl K: Metformin selectively targets cancer stem cells, and acts together with chemotherapy to block tumor growth and prolong remission. *Cancer Res* **69**, 7507–7511, 2009. doi:10.1158/0008-5472.CAN-09-2994.
35. Bednar F, and Simeone DM: Metformin and cancer stem cells: old drug, new targets. *Cancer Prev Res (Phila)* **5**, 351–354, 2012. doi: 10.1158/1940-6207.CAPR-12-0026.
36. Tahermansouri H, and Abedi E: One-pot functionalization of short carboxyl multi-walled carbon nanotubes with ninhydrin and thiourea via microwave and thermal methods and their effect on MKN-45 and MCF7 cancer cells. *Fullerenes Nanotubes Carbon Nanostruct* **22**, 834–844, 2014.
37. Wang L, Shi J, Zhang H, Li H, Gao Y, et al. Synergistic anticancer effect of RNAi and photothermal therapy mediated by functionalized single-walled carbon nanotubes. *Biomaterials* **34**, 262–274, 2013.
38. Cataldo F: A study on the action of ozone on multi-wall carbon nanotubes. *Fullerenes Nanotubes Carbon Nanostruct* **16**, 1–17, 2008.
39. Singh P, Ménard-Moyon C, Battigelli A, Toma FM, Raya J, et al. Double functionalization of carbon nanotubes with purine and pyrimidine derivatives. *Chem Asian J* **8**, 1472–1481, 2013. doi: 10.1002/asia.201300116.
40. Heidari A, Beheshty MH, and Rahimi H: Functionalization of multi-walled carbon nanotubes via direct friedel-crafts acylation in an optimized PPA/P2O5 medium. *Fullerenes Nanotubes Carbon Nanostruct* **21**, 516–524, 2013.
41. Azizian J, Tahermansouri H, Chobfrosh Khoei D, Yadollahzadeh K, and Delbari AS: Microwave-induced chemical functionalization of carboxylated multi-walled nanotubes with 2,3-diaminopyridine. *Fullerenes. Nanotubes and Carbon Nanostruct* **20**, 183–190, 2012.
42. Tahermansouri H, Islami F, Gardaneh M, and Kiani F: Functionalisation of multiwalled carbon nanotubes with thiazole derivative and their influence on SKBR3 and HEK293 cell lines. *Materials Technology: Advanced Performance Materials* **31**, 371–376, 2016.
43. Gharib E, Gardaneh M, and Shojaei S: Upregulation of glutathione peroxidase-1 expression and activity by glial cell line-derived neurotrophic factor promotes high-level protection of PC12 cells against 6-hydroxydopamine and hydrogen peroxide toxicities. *Rejuvenation Res* **16**, 185–199, 2013. doi: 10.1089/rej.2012.1390.
44. Esmailzadeh E, Gardaneh M, Gharib E, and Sabouni F: Shikonin protects dopaminergic cell line PC12 against 6-hydroxydopamine-mediated neurotoxicity via both glutathione-dependent and independent pathways and by inhibiting apoptosis. *Neurochem Res* **38**, 1590–1604, 2013. doi: 10.1007/s11064-013-1061-9.
45. Gardaneh M, Gholami M, and Maghsoudi N: Synergy between glutathione peroxidase-1 and astrocytic growth factors suppresses free radical generation and protects dopaminergic neurons against 6-hydroxydopamine. *Rejuvenation Res* **14**, 195–204, 2011. doi: 10.1089/rej.2010.1080.
46. Gardaneh M, Shojaei S, Kaviani A, and Behnam B: GDNF induces RET-SRC-HER2-dependent growth in

- trastuzumab-sensitive but SRC-independent growth in resistant breast tumor cells. *Breast Cancer Res Treat* **162**, 231–241, 2017. doi: [10.1007/s10549-016-4078-3](https://doi.org/10.1007/s10549-016-4078-3).
47. Burnett JP, Korkaya H, Ouzounova MD, Jiang H, Conley SJ, et al. Trastuzumab resistance induces EMT to transform HER2(+) PTEN(-) to a triple negative breast cancer that requires unique treatment options. *Sci Rep* **5**, 15821, 2015. doi:[10.1038/srep15821](https://doi.org/10.1038/srep15821).
  48. Chen TW, Liang YN, Feng D, Tao LY, Qi K, et al. Metformin inhibits proliferation and promotes apoptosis of HER2 positive breast cancer cells by downregulating HSP90. *J BUON* **18**, 51–56, 2013.
  49. Deng XS, Wang S, Deng A, Liu B, Edgerton SM, et al. Metformin targets Stat3 to inhibit cell growth and induce apoptosis in triple-negative breast cancers. *Cell Cycle* **11**, 367–376, 2012. doi: [10.4161/cc.11.2.18813](https://doi.org/10.4161/cc.11.2.18813).
  50. Li Y, Wang M, Zhi P, You J, and Gao JQ: Metformin synergistically suppress tumor growth with doxorubicin and reverse drug resistance by inhibiting the expression and function of P-glycoprotein in MCF7/ADR cells and xenograft models. *Oncotarget* **9**, 2158–2174, 2017. doi:[10.18632/oncotarget.23187](https://doi.org/10.18632/oncotarget.23187).
  51. Chung YC, Chang CM, Wei WC, Chang TW, Chang KJ, et al. Metformin-induced caveolin-1 expression promotes T-DM1 drug efficacy in breast cancer cells. *Sci Rep* **8**, 3930, 2018. doi:[10.1038/s41598-018-22250-8](https://doi.org/10.1038/s41598-018-22250-8).
  52. Cioce M, Valerio MC, Casadei L, Pulito C, Sacconi A, et al. Metformin induced metabolic reprogramming of chemoresistant ALDH bright breast cancer cells. *Oncotarget* **5**, 4129–4143, 2014.
  53. Vazquez-Martin A, Oliveras-Ferraros C, Cufi S, Del Barco S, Martin-Castillo B, et al. Metformin regulates breast cancer stem cell ontogeny by transcriptional regulation of the epithelial-mesenchymal transition (EMT) status. *Cell Cycle* **9**, 3807–3814, 2010.
  54. Cufi S, Corominas-Faja B, Vazquez-Martin A, Oliveras-Ferraros C, Dorca J, et al. Metformin-induced preferential killing of breast cancer initiating CD44 + CD24-/low cells is sufficient to overcome primary resistance to trastuzumab in HER2+ human breast cancer xenografts. *Oncotarget* **3**, 395–398, 2012.
  55. Liu B, Fan Z, Edgerton SM, Yang X, Lind SE, and Thor AD: Potent antiproliferative effects of metformin on trastuzumab-resistant breast cancer cells via inhibition of ErbB2/IGF-1 receptor interactions. *Cell Cycle* **10**, 2959–2966, 2011.
  56. Anisimov VN, Berstein LM, Egormin PA, Piskunova TS, Popovich IG, et al. Effect of metformin on life span and on the development of spontaneous mammary tumors in HER-2/neu transgenic mice. *Exp Gerontol* **40**, 685–693, 2005.
  57. Anisimov VN, Egormin PA, Piskunova TS, Popovich IG, Tyndyk ML, et al. Metformin extends life span of HER-2/neu transgenic mice and in combination with melatonin inhibits growth of transplantable tumors in vivo. *Cell Cycle* **9**, 188–197, 2010.
  58. Zhu P, Davis M, Blackwelder AJ, Bachman N, Liu B, et al. Metformin selectively targets tumor-initiating cells in ErbB2-overexpressing breast cancer models. *Cancer Prev Res (Phila)* **7**, 199–210, 2014. doi:[10.1158/1940-6207.CAPR-13-0181](https://doi.org/10.1158/1940-6207.CAPR-13-0181).